Probabilistic Engineering Mechanics 7 (1992) 75–89

Numerical simulation of Burgers' turbulence revisited

B. Sefik

Department of Theoretical and Applied Mechanics Faculty of Sciences, Technical University of Istanbul, Maslak, Istanbul, 80626, Turkey

& C.I. Christov

Laboratory of Hydrometeorological Informatics, Hydrometeorological Service, Bulgarian Academy of Sciences, boul. Lenin 66, Sofia, 1184, Bulgaria

(Received October 1989; accepted May 1991)

The stochastic solution to the Burgers' equation evolving from a random initial condition is obtained numerically by means of a conservative difference scheme. The performance of the scheme is checked by means of a number of mandatory numerical tests involving different mesh sizes. Various multi-point statistical characteristics, e.g. three-point third-order correlation and two-point third- and fourth-order correlations, are calculated from the random solution and shown graphically. The results for the correlation function and normalized spectrum are compared with earlier findings from numerical simulations of other authors performed with different numerical techniques and the agreement is quantitatively very good. A kind of stochastic self-similarity is observed for large times. In the end the usefulness of the data gathered is demonstrated through comparing the results for the statistical properties from the direct numerical simulation with the predictions of so-called 'random-point approximation' and the agreement turns out to be fully satisfactory.

1 INTRODUCTION

In the last couple of decades a number of different stochastic models of turbulence (or in more broad sense — of chaotic dynamics) has appeared and unlike the classical semiempirical theories these new models are devised to give predictions not only for local average characteristics but also for multi-point statistical characteristics (moments, cumulants, spectra, etc.), e.g. for the third- or fourth-order generalized correlations functions (cumulants). We cite here just the most frequently used among these approaches.

The first approach is the so-called zero fourth-order cumulant approximation originated by Millionshchikov[1] and developed independently by Proudman & Reid[2] and Tatsumi.[3] It is instructive to point out that the first application of that approach was to the Burgers' equation.[4] After Ogura[5] pointed out the flaws with the energy spectrum for moderate Reynolds numbers the said approach was modified by Tatsumi & Tokunaga[6] and by Tatsumi *et al.*[7]

An approach which is capable of predicting the multi-point statistical characteristics is the Wiener–Hermite method that stemmed from the idea of Wiener to develop a random function into functional series with respect to the Brownian motion process.[8] It was developed by Siegel *et al.*[10] and Meecham & Siegel[11] (see also Hodge & Meecham[12] and Khang & Siegel[13]).

Another approach of the said type is the Lagrangian-history direct-interaction approximation of Kraichnan.[14]

Finally we mention also the recently developed authors' work 'random point approximation' which is akin to the Wiener–Hermite method with the main difference that instead of the Wiener process the basis function of the functional series is chosen to be the Poissonian random function or more generally — a marked random point function. A review and a brief discussion on the random point approximation are given in Section 5 of the present paper. The choice of random point basis function brings the series close to the physical nature of the processes and as a result the convergence is improved.

Probabilistic Engineering Mechanics 0266-8920/92/$05.00

The latter is materialized in the fact that the truncated series here do not require normalization for large times as the Wiener–Hermite method does.[15]

Naturally, for the real-turbulence cases the above listed methods even for the first-order kernels result in large three-dimensional systems of partial differential equations which are very difficult to solve numerically in order to obtain the quantitative predictions. For this reason model equations are sought to be treated by the respective techniques. One of the most popular in this instance is the Burgers' equation which has constantly been a test example when developing all the above mentioned stochastic models. Even the recently developed subgrid models of turbulence were initially tested for the case of Burgers' turbulence (see, for example, Love[16]).

The proper verification of the cited models requires experimental data for the higher- order multi-point average quantities to compare with. This is the reason for revisiting the numerical simulation of Burgers' turbulence and to compile for the various statistical characteristics additional data, which are not present in the above cited earlier numerical simulations of the Burgers' turbulence.

2 BURGERS' EQUATION

Burgers[17] introduced the equation

$$\frac{\partial u}{\partial t} + u\frac{\partial u}{\partial x} = v\frac{\partial^2 u}{\partial x^2} \tag{1}$$

as a substitute for the full Navier–Stokes system for the case when one-dimensional shock waves in slightly compressible viscous fluid are considered. Here u is velocity, v the kinematic viscosity coefficient. Even in the simplest one-dimensional case the precise model for propagation of weak shock waves in slightly compressible liquids requires taking into account also the continuity equation. It is interesting to mention, however, that the stochastic characteristics obtained from that more complicated model[18] are essentially the same as those obtained from the mere Burgers' equation as reported by Jeng *et al.*[19]

The Burgers' equation retains the major features of the full system, namely, the nonlinearity and viscosity, while being at the same time much simpler. The only disadvantage of using the Burgers' equation is that it is hard to find a physically meaningful experimental situation quantitatively relevant to the Burgers' equation. As a result the only way to gather data concerning the statistical characteristics of the random regimes governed by the Burgers' equation is the direct numerical simulation. Due to the dissipative properties of the Burgers' equation a spontaneous generation of disturbances is not observed and the random regime can be provoked by a random loading or random initial condition. In the former case the statistics of the random solution depend heavily on the statistics of loading which can obscure the manifestation of the intrinsic properties of the equation. For this reason we consider the so-called 'initial-condition Burgers' turbulence' and call it for the sake of brevity 'Burgers' turbulence'. As it shall turn out henceforth the initial condition is soon 'forgotten' and the solution reaches a stage of stochastic similarity, which property is especially convenient for checking various models. The latter is one more justification for considering the evolution of a solution of the Burgers' equation from a random initial condition.

The first simulation of Burgers' turbulence was reported by Jeng *et al.*[19] who implemented numerically the transformation of Hopf[20] and Cole.[21] Giorgini[22] also conducted a numerical experiment with the initial condition Burgers' turbulence but by means of Fourier method. The findings of Jeng *et al.*[19] were essentially confirmed by Tokunaga[18] and form now a firm basis for further investigation in this direction. The necessity of such investigations is obvious in the light of what has been said above in that the recently developed stochastic models are capable of predicting more sophisticated statistical characteristics at a time when the numerical experiment of Jeng *et al.*[19] provides data only for the correlation function and the spectrum, the latter being derived from the former. Among other results Giorgini[22] also reports the correlation function and spectrum, and the former is not in good agreement with that of Jeng *et al.*[19]

The present paper deals with repeating the numerical simulation of Burgers' turbulence for the purposes of compiling data concerning various multi-point correlation functions (cumulants) and multi-spectra. We employ a difference approximation to the Burgers' equation which has the obvious advantage over the Hopf–Cole transformation of not requiring evaluation of integrals from exponents for each grid point. The disadvantage is also obvious and is connected with the inevitable occurrence, for difference schemes, of artificial viscosity the latter introduced by the approximation of the nonlinear terms (see, for example, Ref. 23). The problems connected with the scheme viscosity are discussed later in the present paper.

Thus our paper contributes one more 'experimental technique' and comparison with the results of Jeng *et al.*[19] obtained by a different 'experimental technique' can prove extremely informative for the intimate properties of the random solution to Burgers' equation.

3 DIFFERENCE SOLUTION TO THE STOCHASTIC INITIAL-BOUNDARY VALUE PROBLEM

Consider the interval $x \in [-L, L]$, where L is a sufficiently large quantity called 'actual infinity'. The said interval is divided into M equal subintervals each of them of length $h = 2L/M$. Hence the positions of grid points are

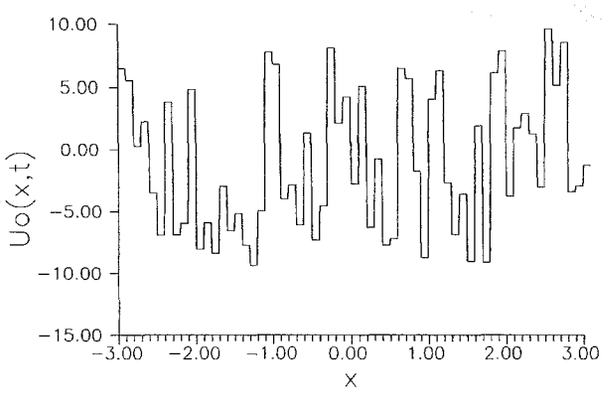

Fig. 1. Shape of the initial condition.

defined as follows

$$x_i = -L + (i - 1)h \qquad i = 1, 2, \ldots, M + 1 \tag{2}$$

Following Jeng *et al.*[19] we consider an initial condition that is a discontinuous function adopting in the different mesh cells $x \in [x_i, x_{i+1}]$ of the uniform mesh random constants as functional values

$$u(x, t_0) = U\beta_i, \qquad |x| \leqslant L \quad \text{for } i = 1, \ldots, M \tag{3}$$

where $U = const.$ is the amplitude of the initial condition and β_i are statistically independent random values with a flat probability distribution in the interval $[-1, 1]$, i.e. $\langle \beta_i \cdot \beta_j \rangle = 0$ for $i \neq j$.

The shape of the initial condition is shown in Fig. 1. Since the initial values of u in different intervals are taken to be independent random numbers the correlation function of the initial condition is a Dirac delta function. Because of discretization one cannot obtain a delta function exactly but only an approximation to the latter. In Fig. 2 the correlation coefficient of the initial condition is depicted (for definitions and difference approximations for the different statistical characteristics see Section 4). It is well seen that this correlation function is virtually equal to zero for all grid intervals except the two that are adjacent to the origin of the co-ordinate system.

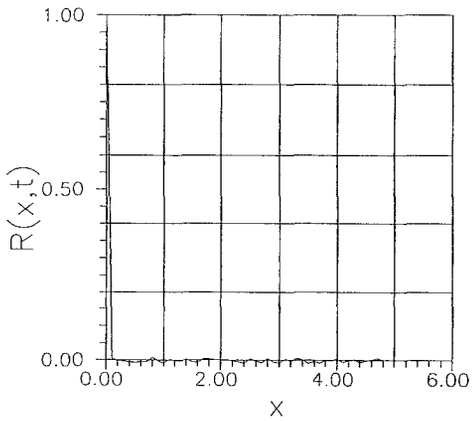

Fig. 2. Correlation of the initial condition.

So, one can conclude that the initial condition is delta-correlated in a numerical sense. This means that the random-numbers generators employed here are adequate.

Concerning the boundary conditions one is faced with a problem in the infinite interval $(-\infty, \infty)$. However, in numerical treatment the region must be finite, say $[-L, L]$, where L is the above introduced large enough value. It has to be several times larger than the distance in which the influence of the boundary condition is diminished. Thus reducing the region by the boundary-adjacent intervals of the said length one has a statistically homogeneous function for which the boundary effects are excluded from consideration.

Provided that the required length L is selected properly, the specific form of the boundary conditions ceases to play any role and we resort therefore to the simplest one

$$u(x, t) = 0, \qquad x = \pm L \tag{4}$$

which is the best in the sense of conservative properties of the difference scheme. There are not any problems in which to use boundary conditions where the first derivatives are equal to zero and we actually did conduct a couple of numerical experiments with those kind of conditions and the results for the averaged statistical characteristics virtually coincided in the inner part of the region with those obtained with boundary condition (4).

A uniform mesh is employed also for the temporal independent variables

$$t_j = t_0 + j\tau \tag{5}$$

where τ is the time increment and t_0 the initial moment of time (set, as a rule, equal to zero).

We use the following conservative and transportive difference scheme for solving eqn (1) (see, for example, Ref. 23)

$$v\left[\frac{u_{i+1}^{j+1} - 2u_i^{j+1} + u_{i-1}^{j+1}}{h^2}\right] - \left[\frac{U_R f_R - U_L f_L}{h}\right] = \frac{u_i^{j+1} - u_i^j}{\tau} \tag{6}$$

where

$$U_R = \frac{u_{i+1}^j + u_i^j}{2} \quad \text{and} \quad U_L = \frac{u_i^j + u_{i-1}^j}{2} \tag{7}$$

$$f_R = \begin{cases} u_i^{j+1}, & U_R > 0 \\ u_{i+1}^{j+1}, & U_R < 0 \end{cases} \quad \text{and}$$

$$f_L = \begin{cases} u_{i-1}^{j+1}, & U_L > 0 \\ u_i^{j+1}, & U_L < 0 \end{cases} \tag{8}$$

for $i = 2, \ldots, M$; and $j = 1, \ldots, N$.

The algebraic system is coupled with the boundary conditions (4) which in terms of set functions recast to

$$u_1^j = 0 \quad \text{and} \quad u_m^j = 0 \quad \text{for } j = 1, \ldots, n \tag{9}$$

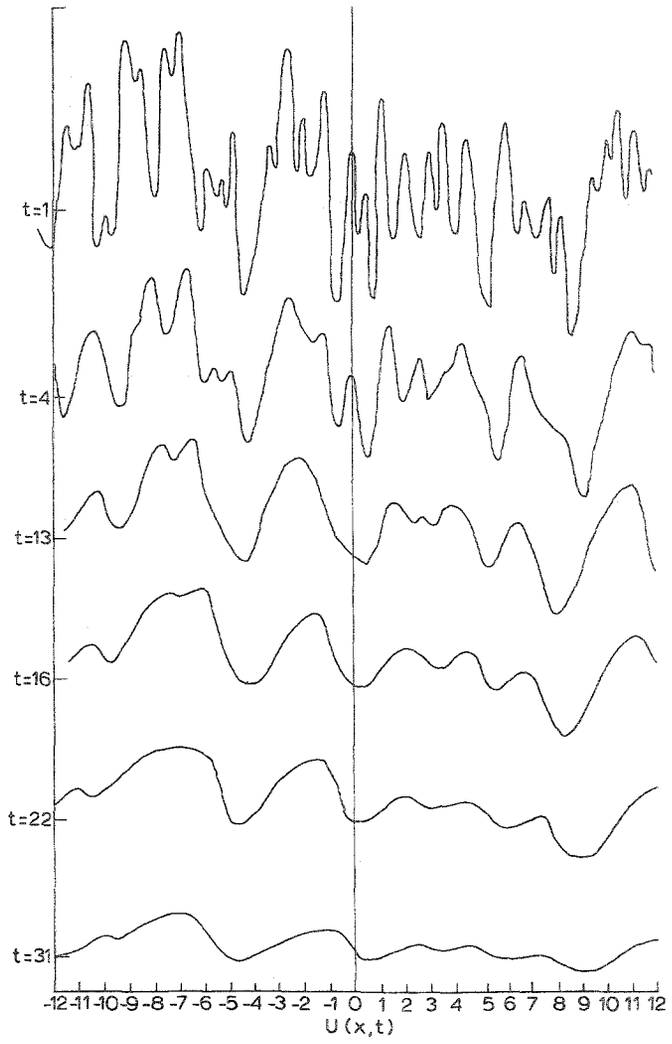

Fig. 3. Evolution with time of the random solution for $v = 1$, $L = 1500$, $h = 0{\cdot}1$, $\tau = 0{\cdot}01$.

So we arrive at a three-diagonal algebraic system with non-dominant main diagonal which is solved by means of Gaussian elimination with pivoting.

The above difference scheme is of second order of approximation in the intervals where the velocity u does not change its sign. It turned out to be stable even for as high as 200 'mesh' Reynolds numbers $Re = Uh/v$, based on the amplitude U of the initial condition.

The evolution of the solution from the initial condition is shown in Fig. 3. As should have been expected, the amplitude of the solution decreases while the characteristic length scale increases. The increase of the length scale is conspicuous also for the correlation function. The evolution with time of the normalized correlation function (correlation coefficient), is shown in Fig. 4 and the effect of 'spreading' is obvious. The interpretation of this phenomena as well as a discussion on the results obtained are in Sections 5 and 6.

Before turning to different statistical characteristics it is obligatory to check the performance of the difference scheme and to verify the convergence of the difference

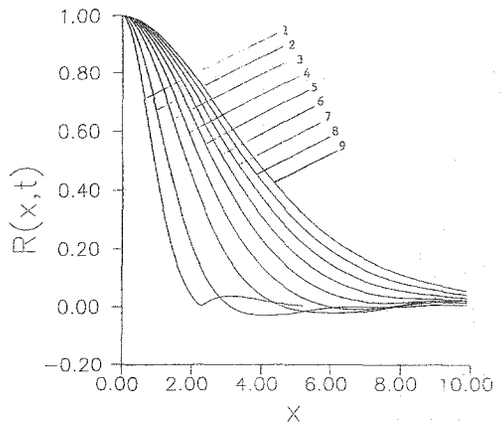

Fig. 4. Evolution with time of the normalized correlation function (correlation coefficient) for $v = 1$, $h = 0{\cdot}1$, $L = 1500$, $L_1 = 1480$, $U = 10$. 1 — $t = -15$; 2 — $t = 00$; 3 — $t = 0{\cdot}3$; 4 — $t = 0{\cdot}6$; 5 — $t = 0{\cdot}9$; 6 — $t = 1{\cdot}2$; 7 — $t = 1{\cdot}5$; 8 — $t = 1{\cdot}8$; 9 — $t = 2{\cdot}1$.

solution to the solution of the differential initial-boundary value problem. As far as a stochastic solution is concerned one cannot compare the actual realizations when deciding upon the quality of the difference scheme but instead comparisons of the average characteristics are to be conducted. For the sake of simplicity we consider in this instance the two-point second-order correlation function.

The interval $2L$ is limited by the capability of the available computer and in our case turns out to be 3000. This value of L is sufficient to harbor a region several times larger than that which one actually needs for calculating the solution statistics. We decided not to run experiments with a decreased value of L and to seek the optimum in the sense of the required computational time since the computational time spent for those experiments might turn out to be comparable with the time needed to perform all calculations with $L = 1500$.

The value h of the spacing appears to be one of the most important parameters of the difference scheme. Formally speaking the difference solution tends to the solution of the original differential equation with $h \to \infty$ and the smaller h is, the better is the approximation. The problem is, however, to find the optimal value for h which secures sufficient accuracy without being excessively small in the light of what has already been said above in the sense that $L = Mh$ must be sufficiently large. Figure 5 presents the results for the correlation coefficient $R(x, t)$ obtained with three different values of h. It is clearly seen that $h = 0{\cdot}1$ is the optimal value since the results for this value and those for $h = 0{\cdot}05$ virtually coincide while the comparison with the case $h = 0{\cdot}2$ shows considerable differences. Henceforth in the present paper all experiments are conducted with $h = 0{\cdot}1$. Here we must mention that the last quantity becomes relatively smaller during evolution of the solution because the characteristic length of the latter increases. In this sense

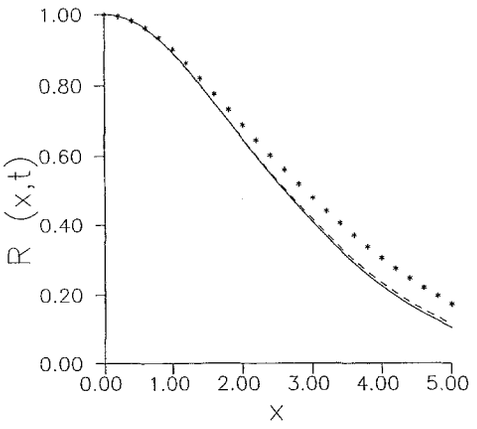

Fig. 5. The correlation coefficient of the solution obtained with three different values of spacing: ***, $h = 0{\cdot}2$; – –, $h = 0{\cdot}1$; ——, $h = 0{\cdot}05$. Here $t = 1{\cdot}2$, $v = 1$, $L = 1500$, $U = 10$.

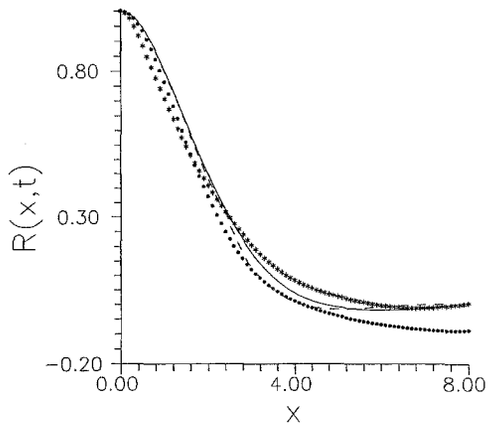

Fig. 6. The correlation coefficient for the solution obtained with three different values of viscosity: ***, $v = 0{\cdot}1$; · · ·, $v = 0{\cdot}4$; – –, $v = 1$; ——, $v = 2$. Here $tv = 0{\cdot}6$, $L = 1500$, $U = 10$.

the practical accuracy of the scheme increases with the increase of time.

The worst shortcoming of the difference approach to solving Burgers' equation consists in the presence of the artificial scheme viscosity introduced by the truncation error that arises when approximating the nonlinear term. Therefore, it is of crucial importance to assess the influence of scheme viscosity. The velocity u decreases with time and hence the artificial viscosity is largest for the initial times when the amplitude of velocity is sufficiently high. Though the high values of the amplitude are limited to the earlier time stages, the scheme viscosity can still affect significantly the solution even for larger times especially when the amplitude of the initial condition is very high. The large scheme viscosity quickly smooths the initial random condition and thus pre-determines the whole evolution of the process. All this means that an optimal selection of values U, v, τ (the value of h has already been set equal to $0{\cdot}1$) is to be found in order to obtain reliable results for the random solution. Marchuk[24] shows that the specific value of the artificial viscosity for implicit schemes of the type considered is

$$v_a = \tfrac{1}{2}(uh + u^2\tau) \tag{10}$$

Here it is to be noted that employing central differences for the first derivatives enables the scheme to be rendered of second order of approximation and the first term for the scheme viscosity vanishes. The problem is, however, that the second-order scheme has its own disadvantage founded in the so-called artificial dispersion connected with the higher-order derivatives proportional to respective powers of h coefficients that enter the differential equation of infinite order to which the considered difference scheme actually corresponds.

The said scheme parameters are interrelated and one of them can be chosen *a priori* and the other fitted in order to decrease the value of the artificial viscosity. We select $U = 10$ which is large enough not to dismantle the nonlinear effects and small enough not to create at the initial time stages an intolerably high value for the artificial viscosity. Three sets of calculations are conducted for $U = 10$ with three different values of the physical coefficient of viscosity v, namely, $v = 0{\cdot}1$, $v = 0{\cdot}4$, $v = 1$, and $v = 2$. Though the highest values of viscosity coefficient v are desirable in order to safely exceed the artificial viscosity, still v is not to be very large because the nonlinearity will be rewarded with a less significant role and that will lead us astray from the main purpose of the present work which aims to investigate the role of interplay between nonlinearity and viscosity when forming the stochastic regime. The results for the correlation coefficient are presented in Fig. 6. It is seen that $v = 1$ is optimal in a sense because the deviation of solution in comparison with the case $v = 2$ is small while the respective deviation with cases $v = 0{\cdot}1$ and $v = 0{\cdot}4$ are considerable. Now we are convinced that $v = 1$ is a proper value for the physical coefficient of viscosity and we remain with that quantity in what follows.

We can neglect the aforesaid if we scale the solution at all time levels with the characteristic velocity U_t which will be defined below.

It is important to compare our findings for the correlation coefficient with the numerical results of Jeng *et al.*[19] (see Fig. 7). The problem is, however, that in that paper neither the exact value of the kinematic coefficient of viscosity v, nor the particular value of time t measured from the moment of initial condition are reported. The initial amplitude U_0 of Jeng *et al.*[19] is also not specified in their work. These difficulties can be avoided to a certain extent through scaling the correlation coefficient by the length scale L_t. Thus the comparison in Fig. 7 has not just a qualitative meaning and is satisfactory beyond any doubts.

4 STATISTICAL CHARACTERISTICS

Let us denote

$$Q(x, t) = \langle u(\xi, t)u(\xi + x, t)\rangle \tag{11}$$

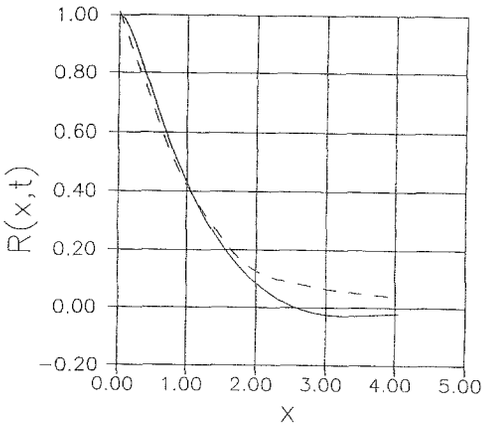

Fig. 7. Comparison with numerical results of Jeng *et al.*[19] for the correlation coefficient: ---, Jeng *et al.*[19] for $t = 0$; ——, present results for $t = 0{\cdot}3$ and $v = 0{\cdot}4$ with co-ordinate x scaled by L_t.

called the correlation function, or simply correlation,

$$Q_{21}(x, t) = \langle u^2(\xi, t)u(\xi + x, t)\rangle \tag{12}$$

$$Q_{12}(x, t) = \langle u(\xi, t)u^2(\xi + x, t)\rangle \tag{13}$$

called two-point third correlations (third cumulants),

$$Q_{111}(x, y, t) = \langle u(\xi, t)u(\xi + x, t)u(\xi + y, t)\rangle \tag{14}$$

called three-point third correlation, and

$$Q_{22}(x, t) = \langle u^2(\xi, t)u^2(\xi + x, t)\rangle \tag{15}$$

$$Q_{13}(x, t) = \langle u(\xi, t)u^3(\xi + x, t)\rangle \tag{16}$$

$$Q_{31}(x, t) = \langle u^3(\xi, t)u(\xi + x, t)\rangle \tag{17}$$

called two-point fourth correlations. In the above formulae $\langle\cdot\rangle$ stands for the statistical (ensemble) averaging. It is clear that in an experiment (e.g. in a numerical experiment) it is much more convenient to compute the time- or spatial-averages. Based upon the ergodicity hypothesis we (among others) shall calculate quantities (11) to (17) as spatial averages, namely

$$Q_{ij}(x, t) = \frac{1}{2L_1}\int_{-L_1}^{L_1} u^i(\xi, t)u^j(\xi + x, t)\,\mathrm{d}\xi$$

$$i, j = 1, 2, 3 \tag{18}$$

$$Q_{111}(x, y, t) = \frac{1}{2L_1}\int_{-L_1}^{L_1} u(\xi, t)u(\xi + x, t)u(\xi + y, t)\,\mathrm{d}\xi \tag{19}$$

where $2L_1$ is the length over which the spatial averaging is taken. Respectively, $x \in \{-L + L_1, L - L_1\}$ and $y \in \{-L + L_1, L - L_1\}$. The above integrals are evaluated numerically by means of the trapezoidal rule. The latter is of second order of approximation with respect to the spacing h, i.e. it safely exceeds the order of approximation of the difference scheme itself.

It is convenient to consider also the normalized correlation functions (in the case of the second-order correlation function Q is is just the correlation coefficient):

$$R_{ij}(x, t) = Q_{ij}(x, t)\,\{\max_x |Q_{ij}(x, t)|\}^{-1}$$

$$\text{for } i, j = 1, 2, 3 \tag{20}$$

$$R_{111}(x, y, t) = Q_{111}(x, y, t)\,\{\max_{x,y} |Q_{111}(x, y, t)|\}^{-1} \tag{21}$$

The energy spectrum is defined as the Fourier transformation of the correlation function

$$E(k, t) = \sqrt{\frac{2}{\pi}}\int_0^\infty Q(x, t)\cos(2k\pi x)\,\mathrm{d}x \tag{22}$$

and the integral in the last formula is evaluated numerically once again by means of the trapezoidal rule according to the scheme:

$$E(\omega_j, t) = \frac{1}{\omega_j}[Q_{m_3}\sin(\omega_j x_{m_3}) - Q_1\sin(\omega_j x_1)] + \frac{1}{h\omega_j^2}\sum_{i=1}^{m_3}\Delta Q\,[\cos(\omega_j x_{i+1}) - \cos(\omega_j x_i)]$$

$$j = 1, \ldots, l \tag{23}$$

where $m_3 = (L - L_1)/h + 1$, $\omega_j = 2\pi k_j$, $\Delta Q = Q(x_{i+1}) - Q(x_i)$ for $i = 1, \ldots, m_3$.

In order to adequately scale the process we introduce (following Jeng *et al.*[19]) the characteristic velocity U_t and characteristic length scale L_t according to formulae

$$U_t = (\langle u^2\rangle)^{1/2} = \sqrt{R(0, t)} \tag{24}$$

$$L_t = \int_0^\infty R(x, t)\,\mathrm{d}x \tag{25}$$

in the first of which it is already acknowledged that the velocity field is a centered stochastic variable. The values of these quantities as functions of time are presented in Table 1.

Table 1. The constants L_t and U_t for different times $v = 1$, $U_0 = 10$

Time	$L_t = \int_0^\infty R(x, t)\,\mathrm{d}x$	$U_t = (\langle u^2\rangle)^{1/2}$
−0·2	1·155	1·703
−1·5	1·047	1·255
0·0	1·347	1·043
0·3	1·861	0·855
0·6	2·224	0·760
0·9	2·916	0·697
1·2	3·317	0·652
1·5	3·682	0·616
1·8	4·014	0·588
2·1	4·314	0·564
2·4	4·585	0·544

5 THE RANDOM-POINT APPROXIMATION, POISSONIAN CASE

The purpose of present work is to gather 'experimental' data for the multi-point statistical characteristics of the

random solution of the Burgers' equation in order to provide a basis for checking and verifying predictions of different 'turbulence' models. Here we consider one of those models: the random point approximation.

In recent years a new point of view on turbulence has evolved according to which along with the small-scale chaotic motions the turbulence signal consists also of organized in a sense (called 'coherent') structures with deterministic average shapes. Occurrence of coherent structures appears to be a general property of nonlinear dynamic systems with chaotic behavior of solution and is now a well recognized phenomenon far beyond the frame of turbulence investigations.

In the author's works, Refs 25–27, a new approach to the random behavior of nonlinear dynamic systems has been originated according to which the predominant part of the random solution is represented by a (generally marked) random point function, composed by structures of similar deterministic shape that are randomly located in the region under consideration (time interval, spatial domain, etc.). The latter is a heuristic assumption based on the observation that the instability gives rise to disturbances that develop and eventually decay returning the system to approximately the same initially unstable state and only after that can a few disturbance occur and the scenario be repeated. During its life span a structure is stable to disturbances of the same characteristic length and the secondary instabilities result in smaller-scale disturbances superimposed upon the main one. The notion of representing the turbulence signal by a random point function fits very well in the picture of a turbulent flow with coherent structures and allows one to obtain self-contained models and to predict quantitatively well the multi-point statistical characteristics of the stochastic regimes for a number of nonlinear systems: Lorenz system,[28,29], Burgers[25–27] and Kuramoto–Sivashinsky[30,31] equations, plane mixing layer,[32–34] near-wall region of plane Poiseuille flow.[35]

There are reasons to believe that even in such a simple dynamic system as the Burgers' equation considered here, the nonlinearity shows itself up through transforming the initial condition of Gaussian-white-noise type into a random train of coherent structures.[26,36] The role of nonlinearity is so significant that it can even generate a random train of structures superimposed on a periodic solution in the case of a stationary Burgers' equation subjected to a periodic load! (see, for instance, Aronson *et al.*[37] and Rabinovich & Suschik[38]).

Before proceeding with details it should be mentioned here that the rigorous generalization of random point approximation goes through the development of the sought for solutions into Volterra–Wiener functional series with marked random point basis function. In the simplest case when a Poissonian random point function is used as a basis function one arrives at the so-called Poisson–Wiener expansion initially considered by Ogura[39] without any applications to particular physical systems. The Poisson–Wiener expansion is akin to the Wiener–Hermite one[10,11] but has a significantly sounder physical basis. In the latter the first-order term represents the Gaussian part of the process and the higher-order terms the deviation from normality. In the former the first-order term represents the contribution of a structure to the random field while the higher-order kernels of the Wiener functionals are interpreted as shape functions of double, triple, etc., interactions among the coherent structures.[27,29,40] Upon acknowledging the viriality of the series under consideration, a natural way to truncate the infinite hierarchy for kernels is to discard the terms after a certain order which yields asymptotically correct results with the respective degree of the number γ of structures per unit length. The latter is not to be said for Wiener–Hermite expansion where the problem for higher-order kernels is not always correct and solving it requires renormalization.[15]

It is clear that the functional series converge faster the closer is the basis function to the function sought and in this instance the Poissonian basis function is more appropriate than the Gaussian one. The convergence can be further improved if more general random point functions are invoked for which the multivariate probability densities are not trivially equal to the respective powers of γ as is the case for the Poissonian random point function.[27,29] If it is done, however, the hard to answer question about the specific shape of these multivariate densities arises and kinetic equations for their evolution are to be derived in a manner which is expected to be rather similar to the way of derivation of the respective densities for multi-particle systems in statistical mechanics (see Ref. 41). Unfortunately, for the time being the 'potential' of interaction of coherent structures is not known. For this reason we resort for the present to the Poissonian basis function and it turns out that it is so well suited to the case of nonlinear stochastic systems that (as shall become clear below) even the very first term in the functional series is capable of giving a good quantitative prediction for the multi-point statistical characteristics for all time stages (including the large times) without any renormalizations.

One should be aware that for the case of Burgers' turbulence the number γ of structures per unit length is a function of time $\gamma = \gamma(t)$ because characteristic length of the process L_t is also a function of time. Before turning to application of the random point approximation one needs to render the dependent and independent variables in a manner so as to have statistical homogeneity of the random solution. Such a procedure is crucial for simplifying the details without obscuring the main idea. In Section 4 it has been mentioned that the characteristic length of the process increases with time. The combination of problem parameters that possess a dimension of length is $\sqrt{vt}$ and starting from certain $t_0 > 0$ one can

without fear of ambiguity scale the variables as follows[27]

$$t = t, \qquad \chi = \frac{x}{\sqrt{vt}}, \qquad u = \sqrt{\frac{v}{k}}\,K(\chi, t) \tag{26}$$

Then

$$\frac{\partial u}{\partial t} = -\frac{1}{2t}\sqrt{\frac{v}{t}}\,K + \sqrt{\frac{v}{t}}\left(-\frac{\chi}{2t}\frac{\partial K}{\partial \chi} + \frac{\partial K}{\partial t}\right)$$

$$\frac{\partial u}{\partial x} = \sqrt{\frac{v}{t}}\frac{1}{\sqrt{vt}}\frac{\partial K}{\partial \chi}$$

$$\frac{\partial^2 u}{\partial x^2} = \frac{1}{vt}\sqrt{\frac{v}{t}}\frac{\partial^2 K}{\partial \chi^2}$$

and introducing these formulae into eqn (1) we arrive at

$$t\frac{\partial K}{\partial t} - \frac{1}{2}\left(K + \chi\frac{\partial K}{\partial \chi}\right) + K\frac{\partial K}{\partial \chi} = \frac{\partial^2 K}{\partial \chi^2} \tag{27}$$

Unlike the solution of eqn (1) the amplitude of the solution of eqn (27) does not decrease with time and one can assume that certain steady and homogeneous values with respect to the spatial variable random process are attained for large times. As shall be seen in the next section, the results of numerical simulation do support that notion. Let us consider then only the stationary case when function K does not depend on time t. Then eqn (27) reduces to following equation

$$-\frac{1}{2}\left(K + \chi\frac{\partial K}{\partial \chi}\right) + K\frac{\partial K}{\partial \chi} = \frac{\partial^2 K}{\partial \chi^2} \tag{28}$$

whose solution can be approximated by a Volterra–Wiener series with respect to the statistically homogeneous Poissonian random density function

$$\psi(\xi) = \sum_{\alpha} \delta(\xi - \chi) \tag{29}$$

with intensity $\varepsilon = \langle\psi(\xi)\rangle = \gamma\sqrt{vt}$ that is a time-independent dimensionless quantity.

It goes far beyond the scope of the present work to discuss the general way of implementing the Volterra–Wiener series (one can catch a feeling of that from author's paper, (Ref. 30)), and for this reason the sketch of random point approximation is confined here just to the first term in the said series, i.e. we seek a solution of eqn (28) in the form

$$K(\chi) = B_0 + \int_{-\infty}^{\infty} B_1(\chi - \xi)[\psi(\xi) - \varepsilon]\,\mathrm{d}\xi \tag{30}$$

It can be shown that the general case is easily reduced to the case of centered random solution for which $B_0''\langle K\rangle = 0$. Moreover the results of Jeng *et al.*[19] and those of the present numerical experiment are concerned exactly with that case. Following the general procedure of kernel identification developed in Christov,[26,27] upon introducing eqn (29) into (30), multiplying by $\psi(0)$ and taking an ensemble average we obtain the following equation for the first-order kernel B_1:

$$-\frac{1}{2}\left(B_1 + \chi\frac{\mathrm{d}B_1}{\mathrm{d}\chi}\right) + B_1\frac{\mathrm{d}B_1}{\mathrm{d}\chi} - \frac{\mathrm{d}^2 B_1}{\mathrm{d}\chi^2} = 0 \tag{31}$$

Equation (31) suggests the main idea of obtaining truncated versions of the hierarchy — neglecting all the kernels of greater than a certain prescribed order. Unlike the Wiener–Hermite method (see also Schetzen,[42] zero-fourth-cumulant approach, local independence assumption (see, for example, Adomian[43])) or other hierarchy techniques (see, for review, Lax[44])) the truncation here bears a profound physical meaning since the higher-order terms are interpreted as the multiple (double, triple, etc.) interactions among the coherent structures, represented by the first-order term.

Boundary conditions reflect the fact that the structures are localized solutions and that the energy of the process is to be finite. In terms of kernels the latter is expressed as follows

$$\int_{-\infty}^{\infty} B_1^2(\chi)\,\mathrm{d}\chi < +\infty \tag{32}$$

and under the natural requirements for smoothness yields to the requirement of decaying the kernels at infinity:

$$B_1(\chi) \to 0, \qquad \chi \to \pm\infty \tag{33}$$

Christov[26] found that a solution of the boundary value problem, eqns (31) and (33), is

$$B_1(\chi) = -\frac{4\chi}{2 + \chi^2} \tag{34}$$

In the frame adopted here, first order approximation of the terms proportional to higher degrees of ε are neglected when the statistical properties are calculated (see Christov[26]) from the random point function and for the different cumulants (see Section 4) the following formula is derived

$$Q_{ij}(x, t) = (-4v)^{i+j}\,\varepsilon^{\min(i,j)}\int_{-\infty}^{\infty}\left[\frac{\xi}{a^2 + \xi^2}\right]^i \times\left[\frac{\xi + x}{a^2 + (\xi + x)^2}\right]^j \mathrm{d}\xi \tag{35}$$

where $a^2 = 2vt$.

The specific technique for calculating the above integrals is presented in the Appendix. Having now the two-point correlation function Q_{11} we evaluate the Fourier transform and obtain the spectrum of energy

$$E(k, t) = \sqrt{\frac{2}{\pi}}\int_0^{\infty} Q_{11}(x, t)\cos(2k\pi x)\,\mathrm{d}x = 4v^2(2\pi)^{3/2}\,\mathrm{e}^{-4\pi}\,|k(2vt)^{1/2}| \tag{36}$$

In the end it is interesting to 'reverse' the use of the random point approximation. Namely, if a flow in which the coherent structures represent the predominant part of the energy is considered then the problem of identification of the structures arises. Assuming that the turbulent field is adequately approximated by a random point function and making use of the well known formula stating that the Fourier transformation of the convolution integral (35) is equal to the product of the

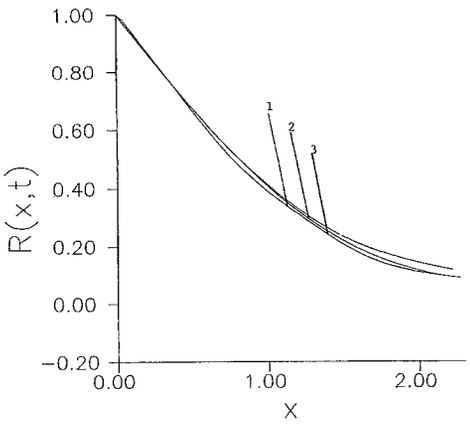

Fig. 8. The self-similarity of the stochastic solution — scaling the average characteristics by the length-scale L_t from eqn (25). The correlation coefficient of Jeng *et al.*[19] 1, $t = 0$; 2, $t = 0{\cdot}75$; 3, $t = 1$.

Fourier transformations of the respective functions under the sign of the integral one derives that the energy spectrum $E(k, t)$ from eqn (36) is simply the square of the modulus of the Fourier transformation (let us call it $D(k, t)$) of function B_1. Then in the case considered of the Burgers' equation when it is known that the kernel sought is an odd function one can identify it from experimental data concerning the spectrum $E(k, t)$ taking the inverse sine-Fourier transformation of function $D(\omega, t) = \sqrt{E(\omega, t)}$, namely

$$B(x, t) = \sqrt{\frac{2}{\pi}} \int_0^\infty D(\omega, t) \sin(\omega x)\, d\omega \qquad (37)$$

In more complicated cases additional information is required in order to identify properly the real and imaginary parts of function D and it is to be discussed elsewhere in a separate paper. The quantitative result from the proposed method of identification is given in the next section.

6 RESULTS AND DISCUSSION

One of the most challenging questions about the random solution to the Burgers' equation is whether a statistical self-similarity exists for large times. The latter can be revealed through scaling the average characteristics by the length-scale L_t from eqn (22). If all of the multipoint correlation functions coincide after the scaling one can speak about self-similarity. Naturally, one cannot go up to correlation functions of infinite order and numerical experiments of the present type can only, more or less, suggest the presence of a self-similarity.

Starting with the results of Jeng *et al.*[19] we have recovered the data from their charts, integrated these data numerically by means of the trapezoidal rule and obtained as a result U_t and L_t. After that the respective functions have been scaled by L_t and the result of that procedure can be seen in Fig. 8. It is obvious that the similarity sought does indeed take place at least for the (second-order) correlation function. It is regretful that the cited results of Jeng *et al.*[19] are available only for a rather sparse set of moments of time: $t = 0$; $t = 0{\cdot}75$; $t = 1$. It is instructive to check the above finding for a more complete population of moments of time. The latter is done in Fig. 9(a) where our results for the scaled (second-order) correlation function are presented. It is obvious that for that function the similarity sought is beyond doubt.

If the similarity is an intrinsic property of the random solution to Burgers' equation then all of the correlation functions should exhibit similarity. The present results strongly suggest that this assertion is true for the first couple of them. In Fig. 9(b) the two-point third-order correlation coefficient $R_{21}(x, t)$ is presented. Here the similarity is obeyed only for moderate distances between the arguments. This is not surprising since the third correlation turns out to be one of the most spoiled quantities in the present numerical experiment. Let us note in passing that its amplitude is rather low and hence it is highly susceptible to truncation and round-off errors of the numerical experiment. Nevertheless, the correspondence between the shapes of the two-point third-order correlation coefficient for different times can be pronounced satisfactory.

Although we can also scale in the same manner the results obtained for the three-point third-order correlation coefficient, we do not present them here because of the inconvenience caused when a multitude of three-dimensional plots is packed onto a single chart. We just mention here that the agreement is essentially the same as in the case of the two-point third-order correlation coefficient shown in Fig. 9(b).

Proceeding along this line we present results for the two-point fourth-order correlation coefficients $R_{13}(x, t)$ in Fig. 9(c) and $R_{22}(x, t)$ in Fig. 9(d). Comparison for different times is very good.

Another not less important indication for similarity of the random solution is the asymptotic behavior of the average characteristics for large times. We focus our attention on the second- and fourth-order quantities: dispersion $Q_{11}(0, t)$ and excess $Q_{22}(0, t)$, respectively, and leave the asymmetry apart because of the above cited reasons concerning the third moments. Table 1 suggests that the length scale L_t grows as $t^{1/2}$ while the characteristic velocity decreases as $t^{-1/2}$ (which compares well with the suggested behavior from the random point approximation outlined in the previous section). The dispersion $Q_{11}(0, t)$ is expected then to decrease as $U_t^2 L_t^{-1}$, i.e. as $t^{-1/2}$. Respectively, the excess $Q_{22}(0, t)$ should behave as $U_t^4 L_t^{-1}$, i.e. as $t^{-3/2}$.

Before all, however, one has to define the 'initial' moment of time for the asymptotic solution in a manner so as to obtain the best fit to the real behavior for large times, i.e. one has to find a real number α for which functions of the type $(t + \alpha)^\kappa$ give the best fit to the

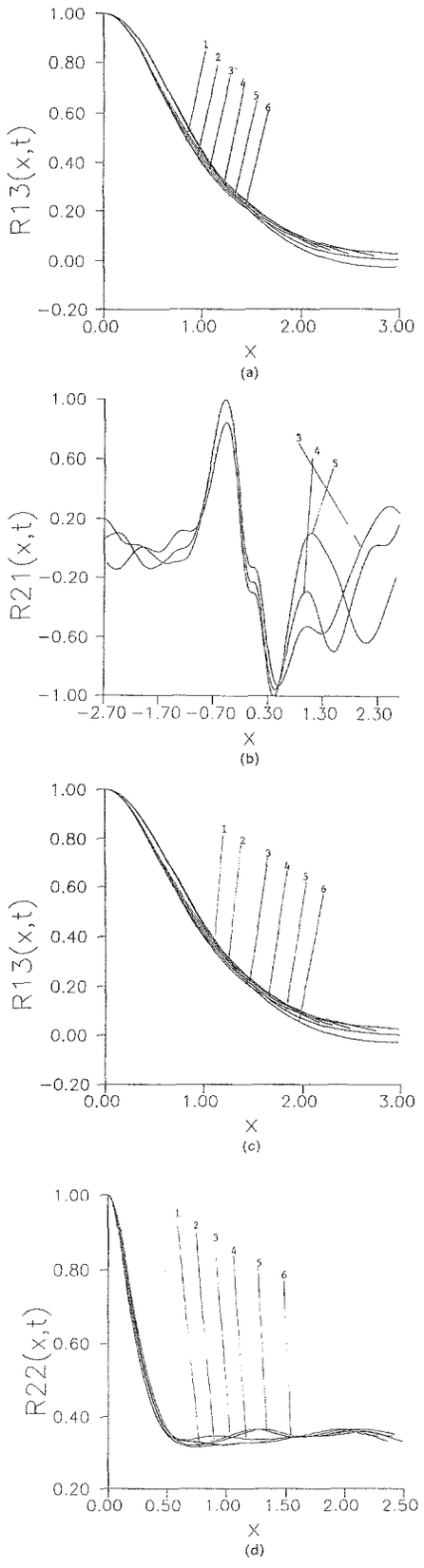

Fig. 9. The self-similarity of the stochastic solution — scaling the average characteristics by the length-scale L_t from eqn (25). Present results for different times: 1, $t = 0{\cdot}3$; 2, $t = 0{\cdot}6$; 3, $t = 0{\cdot}9$; 4, $t = 1{\cdot}2$; 5, $t = 1{\cdot}5$; 6, $t = 1{\cdot}8$. (a) The correlation coefficient $R_{13}(x, t)$; (b) the two-point third-order correlation coefficient $R_{21}(x, t)$; (c) the two-point fourth-order correlation coefficient $R_{13}(x, t)$; (d) the two-point fourth-order correlation coefficient $R_{22}(x, t)$.

Table 2. The constants $\langle u^2 \rangle$ and $\langle u^4 \rangle$ for different times $v = 1{\cdot}0$, $U_0 = 10$

Time	$\langle u^2 \rangle$	$\langle u^4 \rangle$
0·0	1·079	3·281
0·3	0·731	1·519
0·6	0·578	0·963
0·9	0·487	0·693
1·2	0·425	0·537
1·5	0·380	0·435
1·8	0·346	0·364
2·1	0·319	0·312
2·4	0·296	0·284

different quantities under consideration. One should be reminded that the asymptotic solution is in fact a result from an initial condition of infinite amplitude imposed in the initial moment of time. Obviously, the numerical solution starts from a finite initial condition and therefore needs some time to straighten out to the asymptotic behavior. In other words, the asymptotic behavior is observed with respect to a certain, 'shifted' time $(t + \alpha)$. The best fit to U_t and L_t gives $\alpha = 0{\cdot}3$ (see Tables 1 and 2 for comparisons). Having thus the value of α defined we compute also the best-fit curves for the dispersion and excess. They are shown in Fig. 10(a) and 10(b), respectively, and compared to the experimental results. It is clearly seen that the expected asymptotic behavior is indeed obeyed by the solution. The particular expressions of the best-fit curves for the two mentioned quantities are

$$Q_{11} = \frac{0{\cdot}5}{\sqrt{v(t + 0{\cdot}30)}} \qquad Q_{22} = \frac{1{\cdot}5}{v(t + 0{\cdot}30)^{3/2}} \tag{38}$$

All that allows us to conclude that the said statistical similarity does exist for the random solution of Burgers' equation. This means that for sufficiently large times we need not distinguish the results for different times but rather that we can consider in view of the ultimate stochastic solution to Burgers' equation just one particular realization of the random solution for a particular value of time. Respectively, scaling the results by the characteristic length L_t we have an invariant basis for comparisons. That being so, the results presented below are scaled accordingly.

In Fig. 11 the above defined two-point higher-order correlation functions $R_{11}(x, t)$, $R_{21}(x, t)$, $R_{13}(x, t)$ and $R_{22}(x, t)$ are shown along with the comparison with the random-point prediction [ ] in Section 5. It is seen that the comparison is very good for the second-order correlation R_{11} and satisfactory for the higher-order correlations. For small correlation distances, however, the comparison is quantitatively good for all functions under consideration. The latter allows us to state once again the conclusion reached in the earlier mentioned

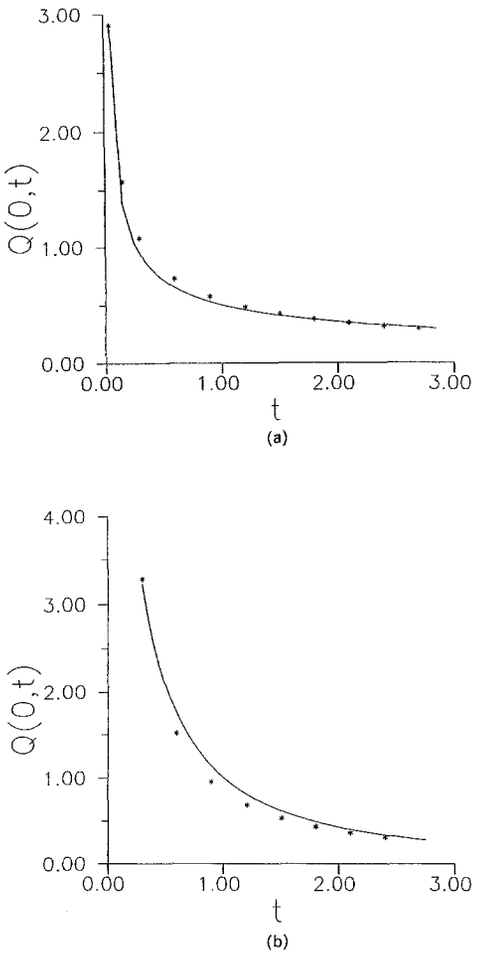

Fig. 10. The self-similarity of the stochastic solution — asymptotic behavior with time: ***, calculations; ——, the curves of best approximation eqn (38). (a) Dispersion $Q_{11}(0, t)$; (b) excess $Q_{22}(0, t)$.

authors' works that the random point approximation even in the Poissonian limit is capable of adequate prediction of the stochastic regime of a nonlinear system as far as moderate correlation distances are considered.

The exhibition of correlations is completed in Fig. 12, which depicts from two different angles the shape of the three-point third-order correlation coefficient for $v = 1$, $t = 1{\cdot}5$, $L = 1500$, $L_1 = 1480$. The comparison with the random point approximation is not presented because of the complications of the chart. It is essentially the same as for the two-point third-order correlation function.

Respectively, in Fig. 13 is shown the spectrum and its comparison to the prediction of random point approximation. Once again the agreement is satisfactory.

In the end we mention some calculations for the probability distributions $P(u)$ of the process and some of its parameters. For example the excess $\langle u^4\rangle/\langle u^2\rangle$ is approximately 2·82 for $t = 0{\cdot}1$, and 2·886 for $t = 0{\cdot}3$ (note that the excess of the initial condition is approximately 1·79) which means that the distribution of the process at a given point is normal while the previous results unequivocally suggest that the two-point distributions are far from Gaussian.

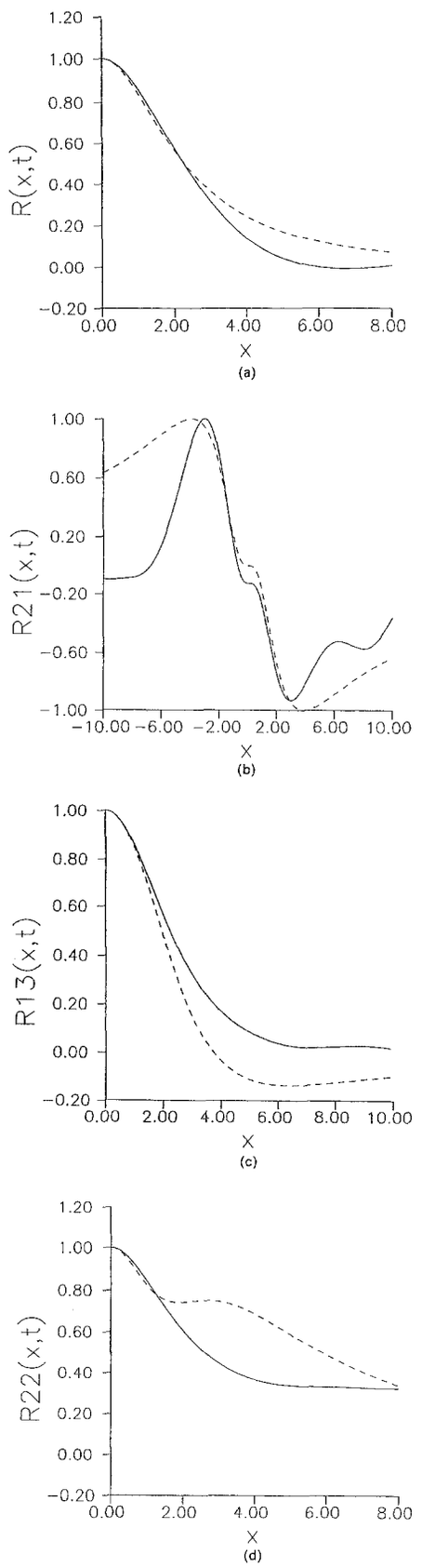

Fig. 11. Comparison between the numerical experiment —— for $v = 1$, $t = 0{\cdot}6$, $L = 1500$, $L_1 = 1480$ and the random-point prediction – – – for $t = 0{\cdot}62$, $v = 1$. (a) The correlation coefficient $R_{11}(x, t)$; (b) the two-point third-order correlation coefficient $R_{21}(x, t)$; (c) the two-point fourth-order correlation coefficient $R_{13}(x, t)$; (d) the two-point fourth-order correlation coefficient $R_{22}(x, t)$.

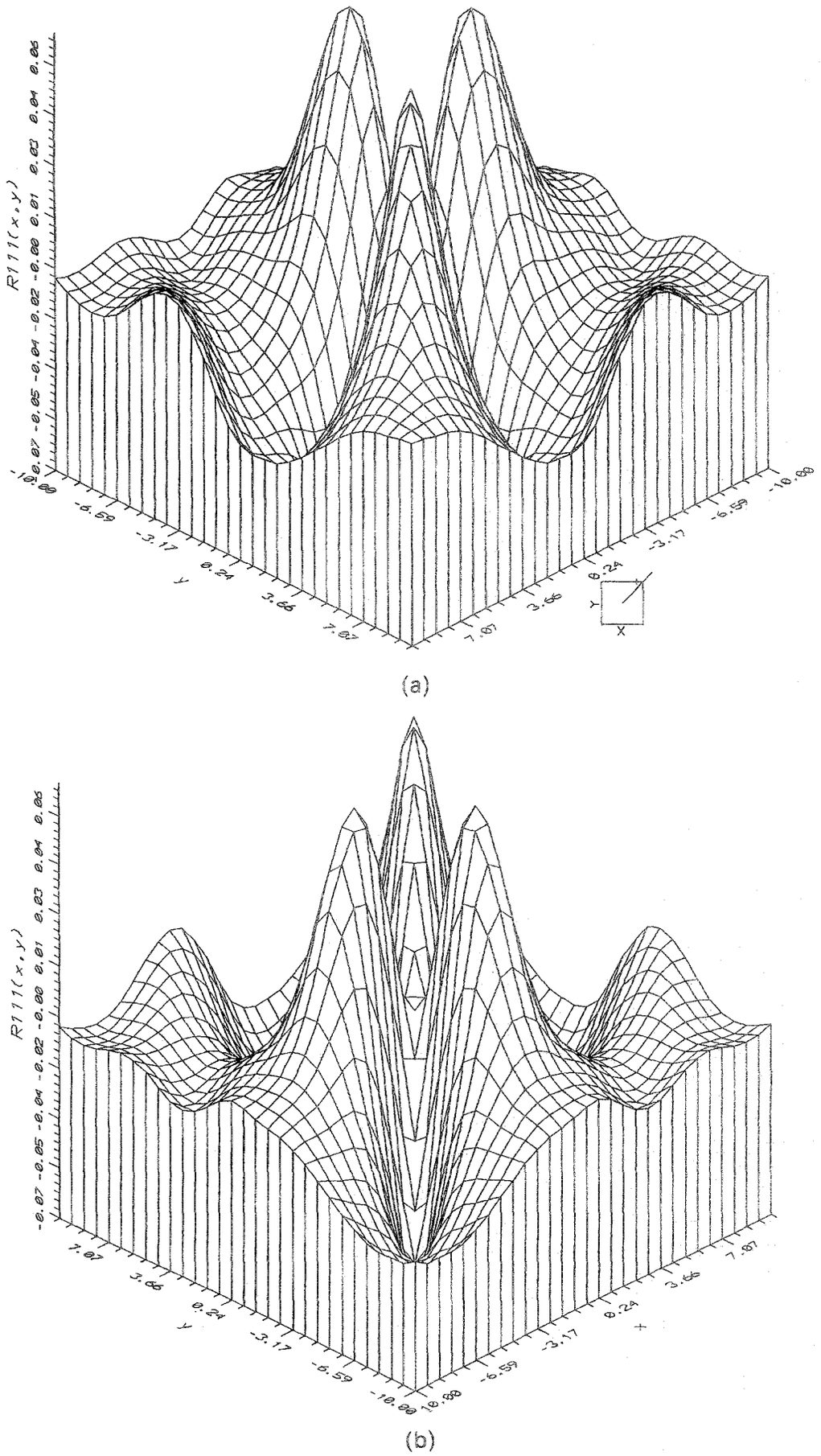

Fig. 12. The shape of the three-point third-order correlation coefficient for $v = 1$, $t = 1{\cdot}5$, $L = 1500$, $L_1 = 1480$ from two different view angles: (a) 45° and (b) 225°.

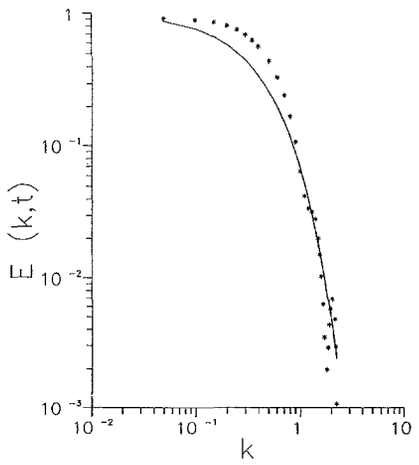

Fig. 13. The spectrum and its comparison to the prediction of random point approximation.

In Fig. 14 we present the particular result from identification of the shape of structures in terms of scaled variables. According to eqn (27) we take the square root of the spectrum and apply consequently the inverse Fourier transform. The agreement with the analytical prediction, eqn (34), is not less than striking. Let us, however, stress that in the case under consideration *a priori* information is available, namely that the structure is an odd function. In general, the identification of the shape of a structure is more complicated and shall be treated elsewhere in a separate paper.

7 CONCLUSIONS

In the present paper a numerical experiment with the initial-condition Burgers' turbulence is performed by means of an implicit difference scheme of first order of approximation with improved convergence. The performance of the numerical technique is verified by means of mandatory tests involving grid-size doubling. As a result, the optimal values of mesh parameters are estimated.

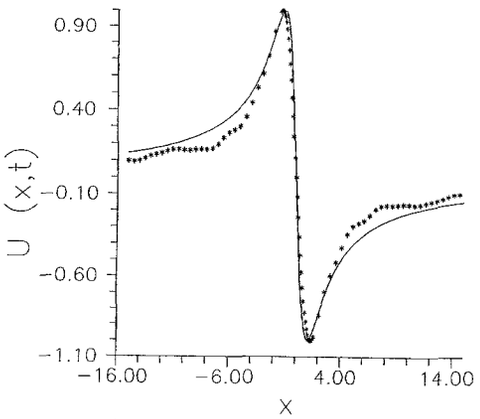

Fig. 14. Identified on the base of eqn (36), the shape of coherent structure (asterisks) is compared with random point approximation (solid line).

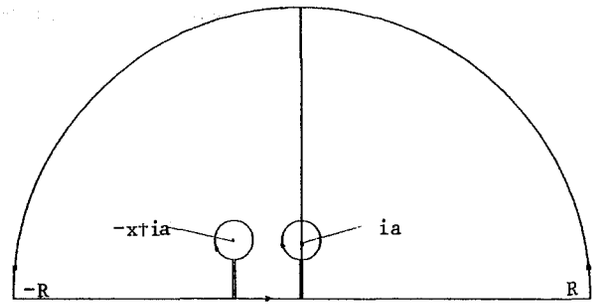

Fig. 15. The region of integration in the complex plane. The singularities whose residues are sought are encircled.

The results obtained strongly suggest that for initial-condition Burgers' turbulence a kind of statistical self-similarity takes place for large times in a sense that the correlation functions up to fourth order preserve their shapes provided that the spatial independent co-ordinate is scaled by a properly defined length scale. The latter is an important finding that enables one to consider only one particular realization of the simulated random function.

The results for multivariate higher-order correlation functions and for the spectrum are compared to the predictions of the so-called random point approximation and the agreement is quantitatively good.

ACKNOWLEDGMENTS

This paper is supported in part by Grant 1052 from the Ministry of Culture Science and Education of Bulgaria.

We wish to thank P.D. Spanos for his advice.

REFERENCES

1. Millionshchikov, M.D., Towards the homogeneous isotropic turbulence. *Com. Rend. Acad. Sci. of the USSR*, **32** (1941) 611–14 and 615–18 (in Russian).
2. Proudman, I. & Reid, W.H., On the decay of normally distributed and homogeneous turbulent velocity fields. *Phil. Trans. Roy. Soc. (London)*, **A247** (1954) 163–89.
3. Tatsumi, T., Theory of isotropic turbulence with the normal joint-probability distribution of velocity. *Proc. 4th Jpn. Natl. Congr. Appl. Mech.*, 1954, pp. 307–11.
4. Reid, W.H., On the transfer of energy in Burgers' model of turbulence. *Appl. Sci. Res.*, **A6** (1957) 85–91.
5. Ogura, Y., A consequence of the zero-fourth-cumulant approximation in the decay of isotropic turbulence. *J. Fluid Mech.*, **16** (1962) 38–49.
6. Tatsumi, T. & Tokunaga, H., One dimensional shock turbulence in a compressible fluid. *J. Fluid Mech.*, **65**(3) (1974) 581–601.
7. Tatsumi, T., Yamada, M. & Takei, T., Factorized cumulant expansion for homogeneous turbulence. *Fluid Dynamics Research*, **1** (1986) 59–75.
8. Wiener, N., *Nonlinear Problems in Random Theory*. Moskva, 1958, (in Russian).
9. Cameron, R.H. & Martin, W.T., The orthogonal development of nonlinear functional series of Fourier–Hermite functional. *Ann. Math. V.*, **48** (1974) 385–92.

10. Siegel, A., Imamura, T. & Meecham, W.C., Wiener–Hermite functional expansion in turbulence with the Burgers' model. *Phys. Fluids*, **6** (1963) 1519–21.
11. Meecham, W.C. & Siegel, A., Wiener–Hermite expansion in model turbulence at large Reynolds numbers. *Phys. Fluids*, **7**(8) (1964) 1178–90.
12. Hodge, H.D. & Meecham, W.C., The Wiener–Hermite expansion applied to decaying isotropic turbulence using a renormalized time-dependent base. *J. Fluid Mech.*, **85**(2) (1978) 325–47.
13. Khang, W.-H. & Siegel, A., The Cameron–Martin–Wiener method in turbulence and in Burgers' model: General formulae, and application to late decay. *J. Fluid Mech.*, **41**(3) (1970) 593–618.
14. Kraichnan, R.H., Lagrangian-history statistical theory for Burgers' equation. *Phys. Fluids*, **11** (1968) 265–77.
15. Meecham, W.C., Renormalization for the Wiener–Hermite representation of statistical turbulence. In *Turbulent Diffusion in Environmental Pollution*, Proc. of a Symp., Charlottesville, Virginia, April 8–14, 1973. *Adv. in Geophys.*, **18a** (1974) 445–55.
16. Love, M.D., Subgrid modelling studies with Burgers' equation. *J. Fluid Mech.*, **100**(1) (1980) 97–110.
17. Burgers, J.M., Correlation problem in one-dimensional model of turbulence. *Proc. Acad. Sci. Amsterdam*, **53** (1950) 247–60.
18. Tokunaga, H., The statistical theory of one dimensional turbulence in a compressible fluid. *J. Phys. Soc. Japan*, **41**(1) (1976) 328–57.
19. Jeng, D.T., Foerster, R., Haaland, S. & Meecham, W.C., Statistical initial-value problem for Burgers' model equation of turbulence. *Phys. Fluids*, **9**(11) (1966) 2114–17.
20. Hopf, E., The partial differential equation u_t 6 $uu_x = \mu u_{xx}$, *Commun. Pure Appl. Math.*, **3** (1950) 201–30.
21. Cole, J.D., On a quasi-linear parabolic equation occurring in aerodynamics. *Quart. Appl. Math.*, **9** (1951) 225–36.
22. Giorgini, A., A numerical experiment on a turbulence model. In *Developments in Mechanics*, Proc. of the Tenth Midwestern Mechanics Conference, Colorado, August 21–23, 1968, p. 1379–1408.
23. Roache, P.J., *Computational Fluid Dynamics*. Hermosa, Albuquerque, N.M., 1972.
24. Marchuk, G.I., *Methods of Computational Mathematics*. Novosibirsk, Nauka — Siberian division, 1973 (in Russian).
25. Christov, C., On a stationary stochastic process of white-noise type with certain special properties. *Bulg. Acad. Sci., Theor. Appl. Mech.*, **10**(1) (1979) 53–7 (in Russian).
26. Christov, C., On a canonical representation for some stochastic processes with application to turbulence. *Bulg. Acad. Sci., Theor. Appl. Mech.*, **11**(1) (1980) 59–66 (in Russian).
27. Christov, C.I., Poisson–Wiener expansion in non-linear stochastic systems. *Ann. de l'Univ. de Sofia, Fac. Math. Mec. Mecanique*, **75**(2) (1981–1982) 143–65.
28. Christov, C.I., On the random-point structure of Lorenz attractor. *Comp. Rend. Acad. Bulg. Sci.*, **40**(4) (1987) 39–42.
29. Christov, C.I., Flows with coherent structures: Application of random point functions and stochastic functional series. *Proc. of the 6th Symposium on Continuum Models and Discrete Systems*, Dijon, 26–30.06.1989. Longman, (in press).
30. Christov, C.I., Stochastic regime for Kuramoto–Sivashinsky equation. Part I: Random-point approximation. *Ann. Univ. Sofia, Fac. Math. Inf. Mechanics*, **81**(2) (1987–1988). (in press).
31. Sefik, B. & Christov, C.I., Stochastic regime for Kuramoto–Sivashinsky equation. Part II: Numerical simulation. *Ann. Univ. Sofia, Fac. Math. Inf. Mechanics*, **81**(2) (1987–1988) (in press).
32. Christov, C.I. Nartov, V.P., On a bifurcation and emerging of a stochastic solution in one variational problem for Poiseuille flows. In *Laminar–Turbulent Transition*, Proc. IUTAM Symposium. Springer, Berlin–Heidelberg, 1985, pp. 227–32.
33. Nartov, V.P., Stochastic regime in mixing layer. Preprint No 24, Institute Theoretical Applied Mechanics, Novosibirsk, 39 pp. (in Russian).
34. Nartov, V.P. & Christov, C.I., *Ann. Univ. Sofia, Fac. Math. Inf. Mechanics*, **81**(2) (1987–1988) (in press, in Russian).
35. Christov, C.I. & Nartov, V.P., On the bifurcation and emerging of a stochastic solution in one variational problem for plane Poiseuille flow. In *Numerical Methods in Viscous Liquid Dynamics*. Novosibirsk, 1984, 124–44 (in Russian). Also in *Dokl. Acad. Sci. USSR*, **277**(4) 825–8.
36. Christov, C.I. & Nartov, V.P., Structural turbulence in MHD flows. In *Physical Mechanics of Heterogeneous Media*. Novosibirsk, 1984, pp. 24–6 (in Russian).
37. Aronson, I.S., Rabinovich, M.I. & Sushchik, M.M., Randomization of coherent structures by a periodic field. In *Chaos and Order in Nature*, ed. H. Haken. Springer, Germany, pp. 54–63.
38. Rabinovich, M.I. & Sushchik, A., Coherent structures in turbulent flows. In *Nonlinear Waves*, ed. A.N. Gaponov–Grekhov. Nauka, Moscow, 1983, pp. 56–85 (in Russian).
39. Ogura, H., Orthogonal functionals of the Poisson process. *IEEE Trans. Inf. Theory*, **18** (1972) 473–81.
40. Christov, C.I. & Sharbanov, B.A. (original name Shefik, B.), An application of the concept of the random point functions for identification of coherent structures in turbulent flows. Int. Conf. COSMEX-89, Tech. Univ. of Wroslaw, Poland, 1989.
41. Bogolyubov, N.N., Problems in dynamic theory in statistical physics. GITTL, Moscow 1946 (in Russian).
42. Schetzen, M. The volterra and Wiener theories of nonlinear systems. John Wiley, New York, 1980.
43. Adomian, G., The closure approximation in hierarchy equations. *J. Stat. Phys.*, **3** (1971) 127–33.
44. Lax, M.D., Approximate solution of random differential and integral equations. In *Applied Stochastic Processes*, ed. G. Adomian. Academic Press, New York–Toronto–Sydney–San Francisco, 1980, pp. 121–34.

APPENDIX

We outline here the way in which an integral of type (35) is solved. Let us begin for definiteness with the case $i = 2$, $j = 2$ which is the most difficult one. In the complex plane the function to be integrated has four poles: $\xi_{1,2} = \pm ia$ and $\xi_{3,4} = -x \pm ia$. Without losing the generality one can consider only the upper half of the plane and to take the integral over the contour depicted in Fig. 15. Its value is equal to the sum of residues in the points of singularity $\xi = ia$ and $\xi = -x + ia$ of the considered complex-valued function $f(z)$.

$$f(z) = \frac{g(z)}{(z - ia)^2} \qquad g(z)$$

$$= \left[\frac{z}{z + ia}\right]^2 \left[\frac{z + x}{a^2 + (z + x)^2}\right]^2$$

Consider the first pole $\xi = ia$. Developing the function $g(z)$ in Taylor series at $z = ia$ the residuum of $f(z)$ at point $z = ia$ is defined as the coefficient of term $(z - ia)^{-1}$:

$$\mathrm{Res}_f(z = ia) = \left.\frac{dg}{dz}\right|_{z=ia} = \frac{1}{4ia}\frac{(x + ia)^2}{(x + 2ia)^2x^2} + \frac{1}{2}\frac{(x + ia)(2a^2 - 2iax - x^2)}{(x + 2ia)^3x^3}$$

Repeating the same procedure for the pole $z = -x + ia$ we obtain

$$\mathrm{Res}_f(z = -x + ia) = \frac{1}{4ia}\frac{(-x + ia)^2}{(x - 2ia)^2x^2} + \frac{1}{2}\frac{(-x + ia)(2a^2 + 2iax - x^2)}{(x - 2ia)^3x^3}$$

Finally, for the fourth-order two-point cumulant we have

$$Q_{22}(x, t) = 2\pi i(-4v)^4\varepsilon^2\,\mathrm{Res}_f(z = x + ia) + \mathrm{Res}_f(z = ia) = \varepsilon^2\frac{256v^4\pi}{(2vt)^{1/2}}\frac{x^4 + 2vtx^2 + 16v^2t^2}{(x^2 + 8vt)^2} \quad \text{(A.1)}$$

In the same manner is obtained

$$Q_{11}(x, t) = \frac{32v^2(2vt)^{1/2}\pi\varepsilon}{(x^2 + 8vt)} \quad \text{(A.2)}$$

$$Q_{21}(x, t) = -Q_{12}(x, t) = -\frac{32v^3\pi x^3\varepsilon}{(2vt)^{1/2}(x^2 + 8vt)^2} \quad \text{(A.3)}$$

$$Q_{13}(x, t) = Q_{31}(x, t) = \frac{32v^4\pi\varepsilon}{(2vt)^{1/2}}\frac{(-3x^4 + 24x^2vt + 128v^2t^2)}{(x^2 + 8vt)^3} \quad \text{(A.4)}$$

$$Q_{111}(x, y, t) = \frac{64v^3\pi\varepsilon}{(2vt)^{-1/2}}\frac{(x + y)(5xy - 2(x^2 + y^2))}{(x^2 + 8vt)(y^2 + 8vt)((y - x)^2 + 8vt))} \quad \text{(A.5)}$$